

Various integral estimations and screening schemes for extended systems in PySCF

Qiming Sun¹

Axiomquant Investment Management LLC, Beijing 100871, China

(*Electronic mail: osirpt.sun@gmail.com)

(Dated: 23 February 2023)

In this document, we briefly review the two-electron integral algorithms based on the range-separated algorithms and Fourier transform integral algorithms that are implemented in the PySCF package. For each integral algorithm, we estimate the upper bound of relevant integrals and derive the necessary conditions for the screening parameters, including distance cutoff and energy cutoff, to reach the desired accuracy. Our numerical tests show that the proposed integral estimators and screening parameters can effectively address the required accuracy while computational efforts are not wasted on unintended accuracy.

I. INTRODUCTION

Gaussian basis with periodic treatments have been made available for extended systems to compute Hartree-Fock, density functional theory (DFT) and post-mean-field methods in various program packages^{1–5}. To characterize periodicity, the Gaussian basis employed by crystalline calculations requires an infinity of primitive Gaussian functions recurrently placed in the repeated image cells. Unlike the integral evaluation program for molecules, evaluating a single crystalline integral involves the computation of massive primitive Gaussian integrals. Thanks to the exponential decay of Gaussian function, given a specific requirement on numerical precision, many primitive integrals can be neglected without breaking the translational symmetry of crystalline integrals. Proper integral screening schemes for extended systems need to be developed to filter the negligible primitive integrals.

For Coulomb-type interactions, integral screening relies on an accurate estimation of electron repulsion integrals (ERI). Integral estimation has big impact on the accuracy and the computational cost in crystalline calculations. Underestimation may cause a loss of accuracy, while overestimation may lead to a waste of computational efforts. Schwarz inequality is the simplest while quite useful integral estimator although it always overestimates the integral value. By including the factor of distance between charge densities, improved Schwarz inequality estimators were proposed in the past^{6–11}. They can be used to screen four-center ERIs and density fitting methods for the bare Coulomb operator and the complementary error function attenuated Coulomb operator^{12,13}.

Integral screening for crystalline integrals is more complex than for molecular integrals due to the presence of periodicity. Crystalline integrals can be evaluated with different integral algorithms^{12,14–31}. Various parameters, such as the range of truncated Coulomb operator, the multipole expansion order, the energy cutoff, the real space grids, etc. have to be used to efficiently compute integrals. It often requires preliminary numerical experiments or certain experience to tune these parameters to achieve desired accuracy without sacrificing performance. Among the crystalline integral evaluation algorithms, Ye developed the range-separated Gaussian density fitting (RSDF) algorithm²⁶ and explored the integral estimators and integral screening scheme for the short-range part of the integrals required by RSDF. His integral estimator helps RSDF algorithm gain a magnitude speed-up comparing to the earlier GDF implementation^{25,26}.

In this work, we document integral estimators and integral screening parameters for the crystalline integral algorithms developed in the PySCF package, including the range-separated density fitting²⁶, the compensated-charge density fitting (CCDF)²⁵, the range-separated exact exchange algorithm (RSJK)²⁹ and the Fourier transform integral algorithm. In Section II, we briefly review these crystalline integral algorithms. In Section III, we discuss the integral estimation and various cutoffs and screening parameters for different types of integrals. The effectiveness of integral screening schemes are assessed in Section IV.

II. INTEGRAL ALGORITHMS IN PYSCF

The periodicity adapted crystalline Gaussian basis is composed of primitive Gaussian functions recurrently placed in N image cells characterized by translational shifts \mathbf{T}

$$\phi_\mu^{\mathbf{k}}(\mathbf{r}) = \frac{1}{\sqrt{N}} \sum_{\mathbf{T}} e^{i\mathbf{k}\cdot\mathbf{T}} \chi_\mu(\mathbf{r} - \mathbf{T}), \quad (1)$$

where $\chi_\mu(\mathbf{r})$ is a primitive Gaussian function centered at \mathbf{R}_μ with normalization factor N_μ

$$\chi_\mu(\mathbf{r}) = N_\mu (x - R_{\mu x})^{m_x} (y - R_{\mu y})^{m_y} (z - R_{\mu z})^{m_z} e^{-\alpha_\mu (\mathbf{r} - \mathbf{R}_\mu)^2}.$$

In an *ab initio* calculation of a crystalline system, essentially one needs to build the overlap integrals and integrals of kinetic operator, nuclear attraction operator, two-electron Coulomb repulsion operator in terms of the crystalline basis.

The translational symmetry allowed overlap integrals between two crystalline basis functions are

$$S_{\mu\nu}^{\mathbf{k}} = \sum_{\mathbf{T}} e^{i\mathbf{k}\cdot\mathbf{T}} S_{\mu\nu\mathbf{T}}, \quad (2)$$

$$S_{\mu\nu\mathbf{T}} = \int \chi_{\mu}(\mathbf{r}) \chi_{\nu}(\mathbf{r} - \mathbf{T}) d^3\mathbf{r}. \quad (3)$$

The lattice-sum over vector \mathbf{T} can be truncated according to the overlap between the two primitive functions $S_{\mu\nu\mathbf{T}}$. We can compute the kinetic integrals in a similar manner.

Nuclear attraction integrals can be computed using the algorithm for three-center two-electron integrals, which we will discuss later. In this treatment, we use a very sharp s-type function to mimic the nuclear charge distribution

$$\chi_A(\mathbf{r}) = Z_A \lim_{\zeta \rightarrow \infty} \left(\frac{\zeta}{2\pi} \right)^{3/2} e^{-\zeta|\mathbf{r} - \mathbf{R}_A|^2} \quad (4)$$

and rewrite the integral of nuclear attraction to

$$V_{N,\mu\nu}^{\mathbf{k}} = \sum_{A \in \text{cell}} \sum_{MN} e^{i\mathbf{k}\cdot(\mathbf{N}-\mathbf{M})} \int \frac{\chi_{\mu}(\mathbf{r}_1 - \mathbf{M}) \chi_{\nu}(\mathbf{r}_1 - \mathbf{N}) \chi_A(\mathbf{r}_2)}{r_{12}} d^3\mathbf{r}_1 d^3\mathbf{r}_2. \quad (5)$$

It is relatively straightforward to compute two-electron Coulomb repulsion integrals with the assistance of plane-waves

$$\frac{e^{i\mathbf{G}\cdot\mathbf{r}}}{\sqrt{2\pi}}. \quad (6)$$

In reciprocal space, the four-center two-electron integrals can be evaluated

$$g_{\mu\nu,\kappa\lambda}^{\mathbf{k}_{\mu}\mathbf{k}_{\nu}\mathbf{k}_{\kappa}\mathbf{k}_{\lambda}} = \frac{1}{\Omega} \sum_{\mathbf{G}} \frac{4\pi \rho_{\mu\nu}^{\mathbf{k}_{\mu}\mathbf{k}_{\nu}}(\mathbf{G} + \mathbf{k}_{\mu\nu}) \rho_{\kappa\lambda}^{\mathbf{k}_{\kappa}\mathbf{k}_{\lambda}}(-\mathbf{G} + \mathbf{k}_{\kappa\lambda})}{|\mathbf{G} + \mathbf{k}_{\mu\nu}|^2}, \quad (7)$$

$$\mathbf{k}_{\mu\nu} = -\mathbf{k}_{\mu} + \mathbf{k}_{\nu}. \quad (8)$$

Ω is the volume of the unit cell. The plane-wave vector \mathbf{G} is chosen to be integer multipliers of reciprocal lattice vectors. The Fourier transformed density (or the product of basis functions) $\rho(\mathbf{G})$ can be obtained with either analytical Fourier transformation

$$\rho_{\mu\nu}^{\mathbf{k}_{\mu}\mathbf{k}_{\nu}}(\mathbf{G}) = \sum_{\mathbf{T}} e^{i\mathbf{k}_{\nu}\cdot\mathbf{T}} \int e^{-i(\mathbf{G}-\mathbf{k}_{\mu\nu})\cdot\mathbf{r}} \chi_{\mu}(\mathbf{r}) \chi_{\nu}(\mathbf{r} - \mathbf{T}) d^3\mathbf{r} \quad (9)$$

or discrete Fourier transformation

$$\rho_{\mu\nu}^{\mathbf{k}_{\mu}\mathbf{k}_{\nu}}(\mathbf{G}) = \frac{1}{\Omega} \sum_{\mathbf{r}} e^{-i(\mathbf{G}-\mathbf{k}_{\mu\nu})\cdot\mathbf{r}} \phi_{\mu}^{\mathbf{k}_{\mu}}(\mathbf{r}) \phi_{\nu}^{\mathbf{k}_{\nu}}(\mathbf{r}). \quad (10)$$

This algorithm can be viewed as a density fitting method using plane-waves as auxiliary basis to expand the electron density. Implementations of this algorithm are available in PySCF with the name FFTDF (fast Fourier transform density fitting) and AFTDF (analytical Fourier transform density fitting).

Computing the two-electron integrals with Fourier transform is expensive in many scenario. Thanks to the locality of Gaussian function in either real space or reciprocal space, recipes that mix real-space and reciprocal-space integral evaluation were developed. They are the range-separated integral algorithms RSDF and RSJK, and the charge-compensated integral algorithm CCDF.

A. Range-separated integral algorithms

Using the error function and its complementary function to split the Coulomb operator

$$\frac{1}{r_{12}} = \frac{\text{erfc}(\omega r_{12})}{r_{12}} + \frac{\text{erf}(\omega r_{12})}{r_{12}}, \quad (11)$$

we get a short-range (SR) component associated with the complementary error function and a long-range (LR) operator associated with the error function. We refer the Coulomb operator with complementary error function to SR because it decays exponentially in real space. In contrast, the LR component has a compact distribution in reciprocal space

$$\frac{4\pi}{G^2} e^{-\frac{G^2}{4\omega^2}}. \quad (12)$$

We also split the electron density into a compact part $\rho_c(\mathbf{r})$ and a diffused part $\rho_d(\mathbf{r})$ based on their compactness in real space. Typically, the diffused part of the density is constructed using smooth Gaussian functions and is expected to be compact in reciprocal space. When computing the two-electron repulsion integrals with the RSJK or RSDF algorithm,

$$\int \frac{\rho(\mathbf{r}_1)\rho(\mathbf{r}_2)}{r_{12}} d^3\mathbf{r}_1 d^3\mathbf{r}_2, \quad (13)$$

locality is utilized and the integrals are computed in two steps. In the first step, we compute the SR Coulomb with the compact density analytically in real space

$$\int \frac{\rho_c(\mathbf{r}_1)\text{erfc}(\omega r_{12})\rho_c(\mathbf{r}_2)}{r_{12}} d^3\mathbf{r}_1 d^3\mathbf{r}_2. \quad (14)$$

For RSJK, computing the four-index analytical integrals requires three nested lattice-sum

$$g_{\mu\nu,\kappa\lambda}^{\mathbf{k}_\mu\mathbf{k}_\nu\mathbf{k}_\kappa\mathbf{k}_\lambda} = \sum_{\mathbf{M}\mathbf{N}\mathbf{T}} e^{i\mathbf{k}_\nu\cdot\mathbf{N}-i\mathbf{k}_\mu\cdot\mathbf{M}-i\mathbf{k}_\kappa\cdot\mathbf{T}} g_{\mu\mathbf{M}\nu\mathbf{N},\kappa\mathbf{T}\lambda} \quad (15)$$

$$g_{\mu\mathbf{M}\nu\mathbf{N},\kappa\mathbf{T}\lambda} = \int \frac{\chi_\mu(\mathbf{r}_1-\mathbf{M})\chi_\nu(\mathbf{r}_1-\mathbf{N})\text{erfc}(\omega r_{12})\chi_\kappa(\mathbf{r}_2-\mathbf{T})\chi_\lambda(\mathbf{r}_2)}{r_{12}} d^3\mathbf{r}_1 d^3\mathbf{r}_2. \quad (16)$$

For RSDF, a single lattice-sum is required for the two-center SR integrals and a double lattice-sum is required for the three-center SR integrals

$$g_{\mu,\nu}^{\mathbf{k}} = \sum_{\mathbf{N}} e^{i\mathbf{k}_\nu\cdot\mathbf{N}} g_{\mu,\nu\mathbf{N}}, \quad (17)$$

$$g_{\mu,\nu\mathbf{N}} = \int \frac{\chi_\mu(\mathbf{r}_1)\text{erfc}(\omega r_{12})\chi_\nu(\mathbf{r}_2-\mathbf{N})}{r_{12}} d^3\mathbf{r}_1 d^3\mathbf{r}_2, \quad (18)$$

$$g_{\mu\nu,\kappa}^{\mathbf{k}_\mu\mathbf{k}_\nu} = \sum_{\mathbf{M}\mathbf{N}} e^{i\mathbf{k}_\nu\cdot\mathbf{N}-i\mathbf{k}_\mu\cdot\mathbf{M}} g_{\mu\mathbf{M}\nu\mathbf{N},\kappa}, \quad (19)$$

$$g_{\mu\mathbf{M}\nu\mathbf{N},\kappa} = \int \frac{\chi_\mu(\mathbf{r}_1-\mathbf{M})\chi_\nu(\mathbf{r}_1-\mathbf{N})\text{erfc}(\omega r_{12})\chi_\kappa(\mathbf{r}_2)}{r_{12}} d^3\mathbf{r}_1 d^3\mathbf{r}_2. \quad (20)$$

In the second step, rest terms, including the LR Coulomb operator or the terms with diffused part of electron density, are all collected and evaluated in reciprocal space numerically, which can be shortly denoted as

$$\frac{1}{\Omega} \sum_{\mathbf{G}} \frac{4\pi}{G^2} \left(\rho(\mathbf{G})\rho(-\mathbf{G}) - (1 - e^{-\frac{G^2}{4\omega^2}}) \rho_c(\mathbf{G})\rho_c(-\mathbf{G}) \right). \quad (21)$$

All terms in this step exhibit a compact distribution in reciprocal space, which allows for rapid truncation of the summation over the plane-wave functions in the formula above. More details of the four-center ERI algorithm can be found in reference 29.

B. Charge-compensated algorithms

In CCDF, we partition the auxiliary basis function into two components, the zero-multipole component and the plane-wave component

$$\varphi_\mu^{\mathbf{k}}(\mathbf{r}) = \frac{1}{\sqrt{N}} \sum_{\mathbf{T}} e^{i\mathbf{k}\cdot\mathbf{T}} [\chi_\mu(\mathbf{r}-\mathbf{T}) - \xi_\mu(\mathbf{r}-\mathbf{T})] + \frac{1}{(2\pi)^3} \sum_{\mathbf{G}} e^{i(\mathbf{G}+\mathbf{k})\cdot\mathbf{r}} \rho_{\xi_\mu}(\mathbf{G}+\mathbf{k}). \quad (22)$$

The zero-multipole function φ is a regular Gaussian function compensated by a smooth Gaussian function ξ that has the same charge (or multipoles). The effect of ξ is eliminated by the plane-wave component

$$\xi_\mu(\mathbf{r}) = \frac{N_\mu}{N_\eta} (x - R_{\mu x})^{m_x} (y - R_{\mu y})^{m_y} (z - R_{\mu z})^{m_z} e^{-\alpha_\mu(\mathbf{r}-\mathbf{R}_\mu)^2}, \quad \eta < \alpha_\mu, \quad (23)$$

$$\rho_{\xi\mu}(\mathbf{G}) = \int e^{-i\mathbf{G}\cdot\mathbf{r}} \xi_\mu(\mathbf{r}) d^3\mathbf{r}. \quad (24)$$

For the two-center and the three-center integrals involving φ , we carry out the analytical integral scheme in real space

$$g_{\mu,v}^{\mathbf{k}} = \sum_{\mathbf{N}} e^{i\mathbf{k}_v \cdot \mathbf{N}} (J_{\mu,v\mathbf{N}} - J_{\xi_\mu,v\mathbf{N}} - J_{\mu,\xi_v\mathbf{N}} + J_{\xi_\mu,\xi_v\mathbf{N}}), \quad (25)$$

$$J_{\mu,v\mathbf{N}} = \int \frac{\chi_\mu(\mathbf{r}_1) \chi_v(\mathbf{r}_2 - \mathbf{N})}{r_{12}} d^3\mathbf{r}_1 d^3\mathbf{r}_2, \quad (26)$$

$$g_{\mu,v,\kappa}^{\mathbf{k}_\mu \mathbf{k}_v} = \sum_{\mathbf{M}\mathbf{N}} e^{i\mathbf{k}_v \cdot \mathbf{N} - i\mathbf{k}_\mu \cdot \mathbf{M}} (J_{\mu\mathbf{M}v\mathbf{N},\kappa} - J_{\mu\mathbf{M}v\mathbf{N},\xi_\kappa}), \quad (27)$$

$$J_{\mu\mathbf{M}v\mathbf{N},\kappa} = \int \frac{\chi_\mu(\mathbf{r}_1 - \mathbf{M}) \chi_v(\mathbf{r}_1 - \mathbf{N}) \chi_\kappa(\mathbf{r}_2)}{r_{12}} d^3\mathbf{r}_1 d^3\mathbf{r}_2. \quad (28)$$

The integrals associated to the plane-wave component are computed in reciprocal space. The formula for the two-center two-electron integrals is

$$\frac{4\pi}{\Omega} \sum_{\mathbf{G}} \frac{\rho_\mu^{\mathbf{k}}(\mathbf{G} + \mathbf{k}) \rho_{\xi_v}^{\mathbf{k}}(-\mathbf{G} - \mathbf{k}) + \rho_{\xi_\mu}^{\mathbf{k}}(\mathbf{G} + \mathbf{k}) \rho_v^{\mathbf{k}}(-\mathbf{G} - \mathbf{k}) - \rho_{\xi_\mu}^{\mathbf{k}}(\mathbf{G} + \mathbf{k}) \rho_{\xi_v}^{\mathbf{k}}(-\mathbf{G} - \mathbf{k})}{|\mathbf{G} + \mathbf{k}|^2} \quad (29)$$

and the formula for the three-center two-electron integrals is

$$\frac{1}{\Omega} \sum_{\mathbf{G}} \frac{4\pi \rho_{\mu v}^{\mathbf{k}_\mu \mathbf{k}_v}(\mathbf{G} + \mathbf{k}_{\mu v}) \rho_\xi(-\mathbf{G} + \mathbf{k}_{\kappa\lambda})}{|\mathbf{G} + \mathbf{k}_{\mu v}|^2}. \quad (30)$$

III. CUTOFFS ESTIMATION

Based on the position of primitive Gaussian functions, we use distance cutoff R_{cut} to determine which image cells to be included in the lattice-sum. For plane-wave functions, we use energy cutoff E_{cut} to truncation the summation of plane-waves.

We first show the conversion between R_{cut} and the range of lattice-sum. Let $\Delta\mathbf{R}$ be the displacement between two atoms in the unit cell. For lattice vectors $\mathbf{a} = (\mathbf{a}_1, \mathbf{a}_2, \mathbf{a}_3)$, $|\mathbf{a}\mathbf{T} + \Delta\mathbf{R}|$ gives the distance between one atom in the reference cell (cell 0) and another atom in the image cell indicated by the vector \mathbf{T} (elements of \mathbf{T} are all integers). Lattice-sum should include all \mathbf{T} s which satisfy

$$|\mathbf{a}\mathbf{T} + \Delta\mathbf{R}| < R_{\text{cut}} \quad (31)$$

Calling QR decomposition for the 3×4 matrix

$$(\mathbf{a}_1, \mathbf{a}_2, \mathbf{a}_3, \Delta\mathbf{R}) = \mathbf{q}\mathbf{c},$$

the inequality (31) can be transformed to

$$(T_x, T_y, T_z, 1) \cdot \mathbf{c}^T \mathbf{c} \cdot \begin{pmatrix} T_x \\ T_y \\ T_z \\ 1 \end{pmatrix} < R_{\text{cut}}^2.$$

This inequality indicates the lower bound and upper bound of T_z

$$T_z^{\text{upper}} = \text{ceil}\left(\frac{R_{\text{cut}} - c_{34}}{c_{33}}\right) \quad (32)$$

$$T_z^{\text{lower}} = \text{floor}\left(\frac{-R_{\text{cut}} - c_{34}}{c_{33}}\right) \quad (33)$$

The lattice-sum along z -direction needs to include all integers in the closed set $[T_z^{\text{lower}}, T_z^{\text{upper}}]$. Similar procedures can be carried out to determine the bound for T_x and T_y as well as the lattice-sum range along x -direction and y -direction.

Given energy cutoff E_{cut} we can determine the minimal number of plane waves \mathbf{N} in each direction with the inequality

$$|\mathbf{N}\mathbf{b}|^2 > 2E_{\text{cut}}. \quad (34)$$

We can find the requirement for N_z with QR decomposition for \mathbf{b}

$$(\mathbf{b}_1, \mathbf{b}_2, \mathbf{b}_3) = \mathbf{q}\mathbf{c}, \quad (35)$$

$$N_z \geq \text{ceil}\left(\frac{\sqrt{2E_{\text{cut}}}}{c_{33}}\right). \quad (36)$$

N_y and N_z can be determined in a similar manner.

A. Distance cutoff for Gaussian basis function on real-space grid

For any grid inside the reference cell, the value of a remote primitive Gaussian function centered at \mathbf{R} has the upper bound

$$\chi_\mu(\mathbf{r} - \mathbf{R}) \leq N_\mu |\mathbf{R}|^{l_\mu} e^{-\alpha_\mu |\mathbf{R}|^2} \quad (37)$$

We can estimate an overall error ε due to a single lattice-sum if neglecting all primitive functions which are placed remoter than R_{cut}

$$\varepsilon = \sum_{|\mathbf{T}| > R_{\text{cut}}} \chi_\mu(\mathbf{r} - \mathbf{T}) \approx \int_{R > R_{\text{cut}}} \chi_\mu(\mathbf{R}) d^3 \mathbf{R} < 4\pi N_\mu \int_{R > R_{\text{cut}}} R^{l_\mu + 2} e^{-\alpha_\mu R^2} dR. \quad (38)$$

To ensure the truncation error smaller than the required precision τ , the value of R_{cut} can be determined by solving the inequality

$$\frac{2\pi N_\mu R_{\text{cut}}^{l_\mu + 1} e^{-\alpha_\mu R_{\text{cut}}^2}}{\Omega \alpha_\mu} < \tau \quad (39)$$

To simplify the estimation for basis functions in the same shell which have the same angular momentum, we approximate the angular part of the normalization factor

$$N_\mu \approx N_R(\alpha_\mu, l_\mu) \sqrt{\frac{2l_\mu + 1}{4\pi}}, \quad (40)$$

where N_R is the radial normalization factor

$$N_R(\alpha_\mu, l_\mu) = \sqrt{\frac{2(2\alpha_\mu)^{l_\mu + 3/2}}{\Gamma(l_\mu + \frac{3}{2})}}. \quad (41)$$

B. Distance cutoff for overlap

Assuming that χ_μ is centered at the coordinate $(0, 0, 0)$, the overlap between two primitive functions χ_μ and χ_ν has an upper limit

$$\begin{aligned} \langle \chi_\mu | \chi_\nu \rangle &\leq N_\mu N_\nu \int x^{l_\mu} (x - |\mathbf{R}_\nu|)^{l_\nu} e^{-\alpha_\mu x^2} e^{-\alpha_\nu (x - |\mathbf{R}_\nu|)^2} e^{-\alpha_{\mu\nu} y^2} e^{-\alpha_{\mu\nu} z^2} dx dy dz \\ &= N_\mu N_\nu \frac{\pi}{\alpha_{\mu\nu}} \int x^{l_\mu} (x - R_\nu)^{l_\nu} e^{-\alpha_\mu x^2} e^{-\alpha_\nu (x - R_\nu)^2} dx. \end{aligned} \quad (42)$$

To simplify the equations, we adopt shorthand notations

$$\alpha_{\mu\nu} = \alpha_\mu + \alpha_\nu, \quad (43)$$

$$l_{\mu\nu} = l_\mu + l_\nu, \quad (44)$$

$$\theta_{\mu\nu} = (\alpha_\mu^{-1} + \alpha_\nu^{-1})^{-1}. \quad (45)$$

We then employ the Gaussian product theorem (GPT)

$$L_{\mu\nu}^k(R) = \sum_{l=0}^k \binom{l_\mu}{l} \binom{l_\nu}{k-l} \left(\frac{\alpha_\nu R}{\alpha_{\mu\nu}}\right)^{l_\mu - l} \left(\frac{-\alpha_\mu R}{\alpha_{\mu\nu}}\right)^{l_\nu + l - k}, \quad (46)$$

and derive the primitive overlap integral

$$I_{\mu\nu} = \pi N_\mu N_\nu e^{-\theta_{\mu\nu} R_\nu^2} \sum_k^{l_{\mu\nu}} L_{\mu\nu}^k(R_\nu) \frac{\Gamma(\frac{k+1}{2})}{\alpha_{\mu\nu}^{(k+3)/2}}. \quad (47)$$

$\Gamma(s) = \Gamma(s, 0)$ is the incomplete gamma function

$$\Gamma(s, t) = \int_t^\infty x^{s-1} e^{-x} dx. \quad (48)$$

By approximating $\Gamma(\frac{k+1}{2}) \approx \sqrt{\pi}$

$$I_{\mu\nu} \lesssim \pi N_\mu N_\nu e^{-\theta_{\mu\nu} R_\nu^2} \sum_k^{l_{\mu\nu}} |L_{\mu\nu}^k(R_\nu)| \frac{\sqrt{\pi}}{\alpha_{\mu\nu}^{(k+3)/2}}, \quad (49)$$

we can factorize the GPT term and obtain the overlap integral upper bound

$$I_{\mu\nu} \lesssim N_\mu N_\nu e^{-\theta_{\mu\nu} R^2} \left(\frac{\alpha_\nu R}{\alpha_{\mu\nu}} + \frac{1}{\sqrt{\alpha_{\mu\nu}}} \right)^{l_\mu} \left(\frac{\alpha_\mu R}{\alpha_{\mu\nu}} + \frac{1}{\sqrt{\alpha_{\mu\nu}}} \right)^{l_\nu} \left(\frac{\pi}{\alpha_{\mu\nu}} \right)^{3/2}. \quad (50)$$

After considering the effect of the single lattice-sum in the overlap integral (2), we derive an approximate value of the truncation error ε

$$\varepsilon < \sum_{|\mathbf{R}| > R_{\text{cut}}} I_{\mu\nu} \approx \frac{4\pi}{\Omega} \int_{R > R_{\text{cut}}} R^2 I_{\mu\nu} dR \approx \frac{2\pi R_{\text{cut}}}{\Omega \theta_{\mu\nu}} I_{\mu\nu} < \tau. \quad (51)$$

Solving this inequality for a specific precision requirement τ , we can obtain R_{cut} for the overlap integrals of crystalline basis.

C. Distance cutoff for Fourier transform

The analytical Fourier transform of Gaussian function product $\chi_\mu \chi_\nu$ is

$$\int e^{-i\mathbf{G} \cdot \mathbf{r}} \chi_\mu(\mathbf{r}) \chi_\nu(\mathbf{r}) d^3 \mathbf{r} = \pi N_\mu N_\nu e^{-\frac{G^2}{4\alpha_{\mu\nu}}} e^{-\theta_{\mu\nu} R^2} \sum_k^{l_{\mu\nu}} L_{\mu\nu}^k(R) \sum_m \binom{k}{m} \frac{(\frac{-iG_\chi}{2\alpha_{\mu\nu}})^{k-m} \Gamma(\frac{m+1}{2})}{\alpha_{\mu\nu}^{(m+3)/2}}. \quad (52)$$

Compared to the overlap integrals, the Fourier transform introduces a factor

$$e^{-\frac{G^2}{4\alpha_{\mu\nu}}} \left(\frac{G}{2\alpha_{\mu\nu}} \right)^n \quad (53)$$

which has a maximum value at

$$\max(e^{-\frac{G^2}{4\alpha_{\mu\nu}}} \left(\frac{G}{2\alpha_{\mu\nu}} \right)^n) = \left(\frac{n}{2e\alpha_{\mu\nu}} \right)^{\frac{n}{2}}. \quad (54)$$

This value can hardly be larger than 1 on a regular Gaussian basis in routine calculations. Therefore, it is sufficient to employ the overlap R_{cut} estimator for analytical Fourier transform.

D. Distance cutoff in RSDF

Density fitting methods require three-center integrals and two-center integrals. We first consider the SR-ERI for three primitive functions based on the multipole expansion estimator developed in Ye's work 26

$$g_{\mu\nu\kappa} = \int \frac{\chi_\mu(\mathbf{r}_1) \chi_\nu(\mathbf{r}_1) \text{erfc}(\omega r_{12}) \chi_\kappa(\mathbf{r}_2)}{r_{12}} d\mathbf{r}_1^3 d\mathbf{r}_2^3$$

$$\lesssim N_\mu N_\nu N_\kappa e^{-\theta_{\mu\nu} d_{\mu\nu}^2} \sum_l^{l_{\mu\nu}} |L_{\mu\nu}^l(d_{\mu\nu})| \frac{\pi^3 v_{l+l_\kappa}(\theta_{\mu\nu\kappa\omega}, R)}{\alpha_{\mu\nu}^{l+3/2} \alpha_\kappa^{l_\kappa+3/2}}, \quad (55)$$

where

$$\theta_{\mu\nu} = (\alpha_\mu^{-1} + \alpha_\nu^{-1})^{-1}, \quad (56)$$

$$\theta_{\mu\nu\kappa\omega} = (\alpha_{\mu\nu}^{-1} + \alpha_\kappa^{-1} + \omega^{-2})^{-1}, \quad (57)$$

$$d_{\mu\nu} = |\mathbf{R}_\mu - \mathbf{R}_\nu|, \quad (58)$$

$$R = |\mathbf{P}_{\mu\nu} - \mathbf{R}_\kappa|, \quad (59)$$

$$\mathbf{P}_{\mu\nu} = \frac{\alpha_\mu \mathbf{R}_\mu + \alpha_\nu \mathbf{R}_\nu}{\alpha_{\mu\nu}}. \quad (60)$$

The notation $d_{\mu\nu}$ is the bra separation (between the centers of χ_μ and χ_ν) and R is the bra-ket separation. The effective potential $v_l(\theta, R)$ has an upper bound

$$v_l(\theta, R) = \frac{\Gamma(l + \frac{1}{2}, \theta R^2)}{\sqrt{\pi} R^{l+1}} \lesssim \frac{(\theta R)^l e^{-\theta R^2}}{\sqrt{\pi} \theta R^2} f_l(\theta R^2), \quad (61)$$

$$f_l(x) = \sum_{k=0}^{l-1} \frac{(2l-1)!!}{(2l-2k-1)!! (2x)^k}. \quad (62)$$

Typically, $1 \leq f_l \lesssim 2$ when the bra-ket separation R is reasonably large. Therefore, we can assume f_l a constant. By applying the factorization similar to the overlap integral (50) we obtain the upper bound of the integral (55)

$$\begin{aligned} g_{\mu\nu\kappa} &\lesssim N_\mu N_\nu N_\kappa e^{-\theta_{\mu\nu} d_{\mu\nu}^2} \left(\frac{\pi^2}{\alpha_{\mu\nu} \alpha_\kappa} \right)^{3/2} \sum_k^{l_{\mu\nu}} |L_{l_\mu, l_\nu}^k(d_{\mu\nu})| \frac{f_{k+l_\kappa}(\theta_{\mu\nu\kappa\omega} R)^{k+l_\kappa} e^{-\theta_{\mu\nu\kappa\omega} R^2}}{\sqrt{\pi} \theta_{\mu\nu\kappa\omega} R^2 \alpha_{\mu\nu}^k \alpha_\kappa^{l_\kappa}} \\ &\leq \frac{Q_{\mu\nu}(R) N_\kappa f_l e^{-\theta_{\mu\nu\kappa\omega} R^2}}{\sqrt{\pi} \theta_{\mu\nu\kappa\omega} R^2} \left(\frac{\pi}{\alpha_\kappa} \right)^{3/2} \left(\frac{\theta_{\mu\nu\kappa\omega} R}{\alpha_\kappa} \right)^{l_\kappa} \\ &\leq \frac{Q_{\mu\nu}(R) N_\kappa f_l e^{-\theta_{\mu\nu\kappa\omega} R^2}}{\sqrt{\pi} \theta_{\mu\nu\kappa\omega} R^2} \left(\frac{\pi}{\alpha_\kappa} \right)^{3/2} \left(\frac{\omega^2 R}{\alpha_\kappa + \omega^2} \right)^{l_\kappa}, \end{aligned} \quad (63)$$

where

$$Q_{\mu\nu}(R) = N_\mu N_\nu e^{-\theta_{\mu\nu} d_{\mu\nu}^2} \left(\frac{\pi}{\alpha_{\mu\nu}} \right)^{3/2} \left(\frac{\alpha_\nu d_{\mu\nu}}{\alpha_{\mu\nu}} + \frac{\theta_{\mu\nu\kappa\omega} R}{\alpha_{\mu\nu}} \right)^{l_\mu} \left(\frac{\alpha_\mu d_{\mu\nu}}{\alpha_{\mu\nu}} + \frac{\theta_{\mu\nu\kappa\omega} R}{\alpha_{\mu\nu}} \right)^{l_\nu}. \quad (64)$$

It is worth noting that $\theta_{\mu\nu\kappa\omega}$ is bounded above

$$\theta_{\mu\nu\kappa\omega} < (\alpha_{\mu\nu}^{-1} + \omega^{-2})^{-1}, \quad (65)$$

and

$$R < 2R_{\text{cut}} \quad (66)$$

because of the distance cutoff which ensures that all primitive Gaussian functions and their products must be inside the sphere of diameter $2R_{\text{cut}}$. By considering these bounds, we obtain the upper bound of $Q_{\mu\nu}(R)$

$$Q_{\mu\nu}^u = N_\mu N_\nu e^{-\theta_{\mu\nu} d_{\mu\nu}^2} \left(\frac{\pi}{\alpha_{\mu\nu}} \right)^{3/2} \left(\frac{\alpha_\nu d_{\mu\nu}}{\alpha_{\mu\nu}} + \frac{2\omega^2 R_{\text{cut}}}{\alpha_{\mu\nu} + \omega^2} \right)^{l_\mu} \left(\frac{\alpha_\mu d_{\mu\nu}}{\alpha_{\mu\nu}} + \frac{2\omega^2 R_{\text{cut}}}{\alpha_{\mu\nu} + \omega^2} \right)^{l_\nu} \quad (67)$$

as well as the upper bound of $g_{\mu\nu\kappa}$

$$g_{\mu\nu\kappa} \lesssim \frac{e^{-\theta_{\mu\nu\kappa\omega} R^2}}{R^2} \frac{Q_{\mu\nu}^u N_\kappa f_l}{\sqrt{\pi} \omega} \left(\frac{\pi}{\alpha_\kappa} \right)^{3/2} \left(\frac{2\omega^2 R_{\text{cut}}}{\alpha_\kappa + \omega^2} \right)^{l_\kappa}. \quad (68)$$

For SR ERIs, the inequality above offers a more accurate upper bound estimation than Schwarz inequality. In the crystalline integral program, we combine the two estimators. Schwarz inequality is tested first for each $g_{\mu\nu\kappa}$ because it is simple and fast to

compute. To reduce the cost of the inequality test (68), we precompute $Q_{\mu\nu}^u$ and the intermediate point center $\mathbf{P}_{\mu\nu}$ then adjust the integral screening threshold for each basis product $\chi_\mu\chi_\nu$. Additionally, $\theta_{\mu\nu\kappa}$ can be precomputed and cached as well because many basis functions have the same exponent and the number of unique $\theta_{\mu\nu\kappa}$ is limited. When computing $g_{\mu\nu\kappa}$, we only require the coordinates of $\mathbf{P}_{\mu\nu}$ and auxiliary basis χ_κ to compute R^2 . Then we test if

$$\frac{e^{-\theta_{\mu\nu\kappa}\omega R^2}}{R^2} \quad (69)$$

is large enough for the adjusted integral screening threshold.

Next we consider the effects of the double lattice-sum in the integral (19). Without loss of generality, we can assume the center of χ_κ being at $\mathbf{0}$. In terms of the exponent part of the primitive three-center integral (55)

$$g_{\mu\nu\kappa} \sim e^{-s}, \quad s = \theta_{\mu\nu}d_{\mu\nu}^2 + \theta_{\mu\nu\kappa}\omega R^2, \quad (70)$$

we can find the asymptotic behaviour for the integral (19)

$$\sum_{\mathbf{M}\mathbf{N}} g_{\mu^{\mathbf{M}}\nu^{\mathbf{N}}\kappa} \sim \sum_{\mathbf{N}} \sum_{\mathbf{M}=\mathbf{N}} e^{-\theta_{\mu\nu}|\mathbf{R}_\mu - \mathbf{R}_\nu|^2} e^{-\theta_{\mu\nu\kappa}\omega|\mathbf{P}_{\mu^{\mathbf{M}}\nu^{\mathbf{N}}}|^2}. \quad (71)$$

This suggests that the contribution from the lattice-sum over \mathbf{M} would decay rapidly, and we can focus on the leading contribution from the lattice sum of \mathbf{N}

$$\sum_{\mathbf{M}\mathbf{N}} g_{\mu^{\mathbf{M}}\nu^{\mathbf{N}}\kappa} \sim \sum_{\mathbf{N}} \max_{\mathbf{R}_\mu} (e^{-\theta_{\mu\nu}|\mathbf{R}_\mu - \mathbf{R}_\nu|^2} e^{-\theta_{\mu\nu\kappa}\omega|\mathbf{P}_{\mu^{\mathbf{M}}\nu^{\mathbf{N}}}|^2}). \quad (72)$$

The double lattice-sum in (19) is reduced to a single lattice-sum. Assuming that the remotest primitive function χ_ν centered at \mathbf{R}_{cut} , approximately the maximum value of $g_{\mu\nu\kappa}$ can be found when the center of primitive function χ_μ is chosen at

$$\mathbf{R}_\mu = \frac{\alpha_{\mu\nu}\alpha_\nu - \alpha_\nu\theta_{\mu\nu\kappa}\omega}{\alpha_{\mu\nu}\alpha_\nu + \alpha_\mu\theta_{\mu\nu\kappa}\omega} \mathbf{R}_{\text{cut}} \quad (73)$$

which minimizes the value of s in (70)

$$s^* = \theta_{\nu\kappa}\omega R_{\text{cut}}^2, \quad \theta_{\nu\kappa}\omega = (\alpha_\nu^{-1} + \alpha_\kappa^{-1} + \omega^{-2})^{-1} \quad (74)$$

with $d_{\mu\nu}$ and R chosen at

$$d_{\mu\nu} = \alpha_\nu^{-1} \theta_{\nu\kappa}\omega R_{\text{cut}}, \quad (75)$$

$$R = \theta_{\mu\nu\kappa}\omega \theta_{\nu\kappa}\omega R_{\text{cut}}. \quad (76)$$

At this configuration, we derive the upper bound of the primitive integral $g_{\mu\nu\kappa}$

$$g_{\mu\nu\kappa} \lesssim \frac{2^{l_\mu} \pi^{5/2} N_\mu N_\nu N_\kappa e^{-s^*} \theta_{\mu\nu\kappa}\omega^{3/2} (\theta_{\nu\kappa}\omega R_{\text{cut}})^{l_{\mu\nu\kappa}-2}}{\alpha_{\mu\nu}^{l_\mu+3/2} \alpha_\kappa^{l_\kappa+3/2} \alpha_\nu^{l_\nu}} f_{l_{\mu\nu\kappa}}(\theta_{\mu\nu\kappa}\omega \theta_{\nu\kappa}\omega R_{\text{cut}}^2), \quad (77)$$

which suggests the distance cutoff estimator for the three-center integral (19)

$$\varepsilon < \frac{1}{\Omega} \int_{R > R_{\text{cut}}} g_{\mu\nu\kappa} d^3 \mathbf{R} \lesssim \frac{2\pi R_{\text{cut}}}{\Omega \theta_{\nu\kappa}\omega} g_{\mu\nu\kappa} < \tau. \quad (78)$$

By carrying out a similar analysis for the two-center primitive SR-ERI, we can approximate its upper bound

$$g_{\mu\nu} \lesssim N_\mu N_\nu \frac{\pi^3 \nu_{l_{\mu\nu}}(\theta_{\mu\nu\omega}, R)}{\alpha_\mu^{l_\mu+3/2} \alpha_\nu^{l_\nu+3/2}}. \quad (79)$$

After considering the lattice summation effect, we get the radial cutoff estimator for the two-center integral (20)

$$\varepsilon \lesssim \frac{2\pi^4 N_\mu N_\nu e^{-\theta_{\mu\nu}\omega R_{\text{cut}}^2} (\theta_{\mu\nu\omega} R_{\text{cut}})^{l_{\mu\nu}-1}}{\Omega \sqrt{\pi \theta_{\mu\nu\omega}} \alpha_\mu^{l_\mu+3/2} \alpha_\nu^{l_\nu+3/2}} < \tau. \quad (80)$$

E. Distance cutoff for RSJK

The four-center primitive SR-ERI has an approximate value

$$g_{\mu\nu\kappa\lambda} = \int \frac{\chi_\mu(\mathbf{r}_1)\chi_\nu(\mathbf{r}_1)\operatorname{erfc}(\omega r_{12})\chi_\kappa(\mathbf{r}_2)\chi_\lambda(\mathbf{r}_2)}{r_{12}} d\mathbf{r}_1^3 d\mathbf{r}_2^3$$

$$\lesssim N_\mu N_\nu N_\kappa N_\lambda e^{-\theta_{\mu\nu} d_{\mu\nu}^2} e^{-\theta_{\kappa\lambda} d_{\kappa\lambda}^2} \sum_k^l \sum_l^{l_{\kappa\lambda}} |L_{l_\mu, l_\nu}^k(d_{\mu\nu}) L_{l_\kappa, l_\lambda}^l(d_{\kappa\lambda})| \frac{\pi^3 v_{k+l}(\theta_{\mu\nu\kappa\lambda\omega}, R)}{\alpha_{\mu\nu}^{k+3/2} \alpha_{\kappa\lambda}^{l+3/2}}, \quad (81)$$

where

$$\theta_{\mu\nu\kappa\lambda\omega} = (\alpha_{\mu\nu}^{-1} + \alpha_{\kappa\lambda}^{-1} + \omega^{-2})^{-1}, \quad (82)$$

$$R = |\mathbf{P}_{\mu\nu} - \mathbf{P}_{\kappa\lambda}|. \quad (83)$$

We then derive the approximation of the upper bound for 4-center SR ERIs

$$g_{\mu\nu\kappa\lambda} \lesssim \frac{Q_{\mu\nu}(R) Q_{\kappa\lambda}(R) f_l e^{-\theta_{\mu\nu\kappa\lambda\omega} R^2}}{\sqrt{\pi \theta_{\mu\nu\kappa\lambda\omega} R^2}}. \quad (84)$$

This estimator can be combined with Schwarz inequality to screen integrals in a manner similar to the 3-center integral screening scheme we discussed in Section III D.

For the triple lattice-sum in the integral (15), it can also be reduced to a single lattice-sum for the similar reason we analyzed in Section III D. The lattice-sum of \mathbf{M} and \mathbf{T} in (19) decays exponentially, and only the lattice-sum of \mathbf{N} needs to be analyzed. Asymptotically,

$$g_{\mu\nu\kappa\lambda} \sim e^{-s}, \quad s = \theta_{\mu\nu} d_{\mu\nu}^2 + \theta_{\kappa\lambda} d_{\kappa\lambda}^2 + \theta_{\mu\nu\kappa\lambda\omega} R^2. \quad (85)$$

Assuming that $\mathbf{R}_\lambda = \mathbf{0}$, the minimal value of s can be found at

$$s^* = \theta_{\nu\lambda\omega} R_\nu^2, \quad \theta_{\nu\lambda\omega} = (\alpha_\nu^{-1} + \alpha_\lambda^{-1} + \omega^{-2})^{-1}, \quad (86)$$

when the positions of function χ_μ and χ_κ are chosen at

$$\mathbf{R}_\mu = \frac{\alpha_{\mu\nu} \alpha_\nu \alpha_\kappa \theta_{\mu\nu\kappa\lambda\omega} - \alpha_{\kappa\lambda} \alpha_\nu \alpha_\lambda \theta_{\mu\nu\kappa\lambda\omega} + \alpha_{\mu\nu} \alpha_\nu \alpha_{\kappa\lambda} \alpha_\lambda}{\alpha_{\mu\nu} \alpha_\nu \alpha_\kappa \theta_{\mu\nu\kappa\lambda\omega} + \alpha_{\kappa\lambda} \alpha_\mu \alpha_\lambda \theta_{\mu\nu\kappa\lambda\omega} + \alpha_{\mu\nu} \alpha_\nu \alpha_{\kappa\lambda} \alpha_\lambda} \mathbf{R}_\nu, \quad (87)$$

$$\mathbf{R}_\kappa = \frac{\alpha_{\mu\nu} \alpha_\nu \alpha_{\kappa\lambda} \theta_{\mu\nu\kappa\lambda\omega}}{\alpha_{\mu\nu} \alpha_\nu \alpha_\kappa \theta_{\mu\nu\kappa\lambda\omega} + \alpha_{\kappa\lambda} \alpha_\mu \alpha_\lambda \theta_{\mu\nu\kappa\lambda\omega} + \alpha_{\mu\nu} \alpha_\nu \alpha_{\kappa\lambda} \alpha_\lambda} \mathbf{R}_\nu. \quad (88)$$

This configuration corresponds to the maximum value of $g_{\mu\nu\kappa\lambda}$ approximately

$$g_{\mu\nu\kappa\lambda} \lesssim \frac{2^{l_{\mu\kappa}} \pi^{5/2} N_\mu N_\nu N_\kappa N_\lambda e^{-s^*} \theta_{\mu\nu\kappa\lambda\omega}^{3/2} (\theta_{\nu\lambda\omega} R_{\text{cut}})^{l_{\mu\nu} + l_{\kappa\lambda} - 2}}{\alpha_{\mu\nu}^{l_{\mu}+3/2} \alpha_{\kappa\lambda}^{l_{\kappa}+3/2} \alpha_\nu^{l_\nu} \alpha_\lambda^{l_\lambda}} f_{l_{\mu\nu\kappa\lambda}} (\theta_{\mu\nu\kappa\lambda\omega}^{-1} \theta_{\nu\lambda\omega}^2 R_{\text{cut}}^2). \quad (89)$$

We then obtain the requirement of R_{cut} for 4-center SR ERIs of RSJK algorithm

$$\frac{2\pi R_{\text{cut}}}{\Omega \theta_{\nu\lambda\omega}} \frac{2^{l_{\mu\kappa}} \pi^{5/2} f_{l_{\mu\nu\kappa\lambda}} N_\mu N_\nu N_\kappa N_\lambda e^{-s^*} \theta_{\mu\nu\kappa\lambda\omega}^{3/2} (\theta_{\nu\lambda\omega} R_{\text{cut}})^{l_{\mu\nu} + l_{\kappa\lambda} - 2}}{\alpha_{\mu\nu}^{l_{\mu}+3/2} \alpha_{\kappa\lambda}^{l_{\kappa}+3/2} \alpha_\nu^{l_\nu} \alpha_\lambda^{l_\lambda}} < \tau. \quad (90)$$

F. Distance cutoff for CCDF

A regular three-center ERI is approximately^{10,11,26}

$$J_{\mu\nu,\kappa} \approx N_\mu N_\nu N_\kappa e^{-\theta_{\mu\nu} d_{\mu\nu}^2} \sum_l L_{l_\mu, l_\nu}^l(d_{\mu\nu}) \frac{\pi^3 (\Gamma(l + l_\kappa + \frac{1}{2}) - \Gamma(l + l_\kappa + \frac{1}{2}, \theta_{\mu\nu\kappa} R^2))}{\alpha_{\mu\nu}^{l_{\mu}+3/2} \alpha_\kappa^{l_{\kappa}+3/2} \sqrt{\pi} R^{l+l_\kappa+1}}. \quad (91)$$

As shown in Eq. (27), the compensated function χ_ξ and the auxiliary function χ_κ are combined when evaluating the analytical three-center integrals

$$J_{\mu\nu,\kappa} - J_{\mu\nu,\xi} \sim \frac{\Gamma(l + l_\kappa + \frac{1}{2}, \theta_{\mu\nu\eta} R^2) - \Gamma(l + l_\kappa + \frac{1}{2}, \theta_{\mu\nu\kappa} R^2)}{R^{l+l_\kappa+1}}, \quad (92)$$

where

$$\theta_{\mu\nu\kappa} = (\alpha_{\mu\nu}^{-1} + \alpha_\kappa^{-1})^{-1}, \quad (93)$$

$$\theta_{\mu\nu\eta} = (\alpha_{\mu\nu}^{-1} + \eta^{-1})^{-1}. \quad (94)$$

In CCDF algorithm, we always have $\theta_{\mu\nu\eta} < \theta_{\mu\nu\kappa}$ because the function χ_ξ is chosen to be the most smooth function. For sufficiently large R , the second Γ function in Eq. (92) is negligible

$$J_{\mu\nu,\kappa} - J_{\mu\nu,\xi} \lesssim N_\mu N_\nu N_\kappa e^{-\theta_{\mu\nu} d_{\mu\nu}^2} \sum_l L_{l_\mu, l_\nu}^l(d_{\mu\nu}) \frac{\pi^3 \Gamma(l + l_\kappa + \frac{1}{2}, \theta_{\mu\nu\eta} R^2)}{\alpha_{\mu\nu}^{l+3/2} \eta^{l_\kappa+3/2} \sqrt{\pi} R^{l+l_\kappa+1}}. \quad (95)$$

Analysis similar to Section IIID can be carried out, which suggests the R_{cut} estimator of the three center integrals (27) for CCDF

$$\frac{2^{l_\mu+1} \pi^{7/2} N_\mu N_\nu N_\kappa e^{-s^*} \theta_{\mu\nu\eta}^{3/2} (\theta_{\nu\eta} R_{\text{cut}})^{l_{\mu\nu\kappa}-2} R_{\text{cut}}}{\Omega \alpha_{\mu\nu}^{l_\mu+3/2} \alpha_\kappa^{l_\kappa+3/2} \alpha_\nu^{l_\nu} \theta_{\nu\eta}} f_{l_{\mu\nu\kappa}}(\theta_{\mu\nu\eta}^{-1} \theta_{\nu\eta}^2 R_{\text{cut}}^2) < \tau \quad (96)$$

where

$$s^* = \theta_{\nu\eta} R_{\text{cut}}^2, \quad (97)$$

$$\theta_{\nu\eta} = (\alpha_\nu^{-1} + \eta^{-1})^{-1}. \quad (98)$$

G. Energy cutoff for four-center Coulomb integrals

The error of a two-electron ERI due to energy cutoff E_{cut} can be estimated

$$\varepsilon(E_{\text{cut}}) = \frac{1}{\Omega} \sum_{|\mathbf{G}|^2 > 2E_{\text{cut}}} \frac{4\pi}{G^2} \rho_{\mu\nu}(\mathbf{G}) \rho_{\kappa\lambda}(-\mathbf{G}) < 16\pi^2 \int_{\sqrt{2E_{\text{cut}}}}^{\infty} \rho_{\mu\nu}(G) \rho_{\kappa\lambda}(G) dG. \quad (99)$$

Based on Eq. (52) the Fourier transform for orbital products, we obtain the leading term of $\rho_{\mu\nu}(G)$

$$\rho_{\mu\nu}(G) = |\rho_{\mu\nu}(\mathbf{G})| \approx N_\mu N_\nu e^{-\frac{G^2}{4\alpha_{\mu\nu}}} e^{-\theta_{\mu\nu} d_{\mu\nu}^2} \left(\frac{G}{2\alpha_{\mu\nu}}\right)^{l_{\mu\nu}} \left(\frac{\pi}{\alpha_{\mu\nu}}\right)^{3/2} \quad (100)$$

Given energy cutoff E_{cut} , the largest error for a density distribution $\rho_{\mu\nu}$ comes with the interaction between $\rho_{\mu\nu}$ and the most compact density $\rho_{\kappa\kappa}$

$$\begin{aligned} \varepsilon(E_{\text{cut}}) &< 16\pi^2 \int_{\sqrt{2E_{\text{cut}}}}^{\infty} \rho_{\mu\nu}(G) \rho_{\kappa\kappa}(G) dG \\ &\approx \frac{16\pi^2 N_\mu N_\nu \theta_{\mu\nu\kappa\kappa} e^{-\theta_{\mu\nu} d_{\mu\nu}^2}}{(2l_\kappa - 1)!! (2\alpha_{\mu\nu})^{l_{\mu\nu}} (4\alpha_\kappa)^{2l_\kappa}} \left(\frac{\pi^2}{2\alpha_{\mu\nu} \alpha_\kappa}\right)^{3/2} (2E_{\text{cut}})^{(l_{\mu\nu} + 2l_\kappa - 1)/2} e^{-\frac{E_{\text{cut}}}{2\theta_{\mu\nu\kappa\kappa}}}. \end{aligned} \quad (101)$$

For the entire system, the energy cutoff error can be derived in terms of the interactions between $\rho_{\kappa\kappa}$ and itself

$$\varepsilon(E_{\text{cut}}) < 16\pi^2 \int_{\sqrt{2E_{\text{cut}}}}^{\infty} \rho_{\kappa\kappa}^2(G) dG. \quad (102)$$

This error estimation then leads to an inequality of E_{cut} with respect to the required precision τ

$$8\pi^2 N_\kappa^4 \left(\frac{\pi}{2\alpha_\kappa}\right)^3 \left(\frac{E_{\text{cut}}}{8\alpha_\kappa^2}\right)^{2l_\kappa-1/2} e^{-\frac{E_{\text{cut}}}{2\alpha_\kappa}} < \tau. \quad (103)$$

It should be noted that the E_{cut} error estimation above is derived with the assumption that the Fourier transform of $\rho_{\mu\nu}(\mathbf{G})$ is analytically computed. If $\rho_{\mu\nu}(\mathbf{G})$ are computed with the fast Fourier transform (FFT) algorithm on N discrete real-space grids

$$\rho_{\mu\nu}(\mathbf{G}) \sim \frac{\Omega}{N} \sum_n^N e^{-i\mathbf{G} \cdot \mathbf{r}_n} \phi_{\mu}^*(\mathbf{r}_n) \phi_{\nu}(\mathbf{r}_n), \quad (104)$$

the E_{cut} estimation (103) is not enough because the error of FFT was not considered. When working on FFT two-electron integrals, one also needs to ensure that the Fourier transform for the orbital product is converged tightly to an error smaller than the required precision. The FFT electron density is

$$\text{FFT}[\rho(\mathbf{r})] = \frac{\Omega}{N} \sum_{n=0}^N e^{-i\mathbf{G} \cdot \mathbf{r}_n} \rho(\mathbf{r}_n), \quad |\mathbf{G}| \leq \sqrt{2E_{\text{cut}}}. \quad (105)$$

We can transform and split the electron density $\rho(\mathbf{r})$ according to the momentum of plane-waves

$$\rho(\mathbf{r}) = \frac{1}{\Omega} \sum_{|\mathbf{G}|=0}^{\infty} e^{i\mathbf{G} \cdot \mathbf{r}_n} \rho(\mathbf{G}) \quad (106)$$

$$= \frac{1}{N} \sum_{G \leq \sqrt{2E_{\text{cut}}}} e^{i\mathbf{G} \cdot \mathbf{r}} \rho(\mathbf{G}) + \frac{1}{N} \sum_{G > \sqrt{2E_{\text{cut}}}} e^{i\mathbf{G} \cdot \mathbf{r}} \rho(\mathbf{G}). \quad (107)$$

The error of FFT electron density is thereby around

$$\text{FFT}[\rho(\mathbf{r})] - \rho(\mathbf{G}) = \left(\frac{1}{N} \sum_{G' n=0}^{\infty} e^{-i\mathbf{G} \cdot \mathbf{r}_n} e^{i\mathbf{G}' \cdot \mathbf{r}_n} \rho(\mathbf{G}') \right) - \rho(\mathbf{G}) \quad (108)$$

$$= \sum_{G' > \sqrt{2E_{\text{cut}}}} \frac{1}{N} \sum_{n=0}^N e^{-i\mathbf{G} \cdot \mathbf{r}_n} e^{i\mathbf{G}' \cdot \mathbf{r}_n} \rho(\mathbf{G}') \quad (109)$$

$$\lesssim \sum_{G' > \sqrt{2E_{\text{cut}}}} \rho(\mathbf{G}'). \quad (110)$$

The error for FFT two-electron integrals can be approximated

$$\varepsilon \approx \frac{1}{\Omega} \sum_{|\mathbf{G}|=0}^{\sqrt{2E_{\text{cut}}}} V(\mathbf{G}) [\text{FFT}[\rho(\mathbf{r})] - \rho(\mathbf{G})] \lesssim v \sum_{G' > \sqrt{2E_{\text{cut}}}} \rho(\mathbf{G}'), \quad (111)$$

where

$$v = \frac{1}{\Omega} \sum_{|\mathbf{G}|=0}^{\sqrt{2E_{\text{cut}}}} V(\mathbf{G}). \quad (112)$$

In practice, we find that the energy cutoff for nuclear attraction integrals (116) is enough to converge the FFT two-electron integrals.

H. Energy cutoff for three-center Coulomb integrals

The Fourier transform for a single Gaussian function is

$$\rho_{\kappa}(\mathbf{G}) = \int e^{-i\mathbf{G} \cdot \mathbf{r}} \chi_{\kappa}(\mathbf{r}) d^3 \mathbf{r} = \pi N_{\kappa} e^{-\frac{G^2}{4\alpha_{\kappa}}} \sum_k \binom{l_{\kappa}}{k} \frac{(\frac{-iG_{\kappa}}{2\alpha_{\kappa}})^{l_{\kappa}-k} \Gamma(\frac{k+1}{2})}{\alpha_{\kappa}^{(k+3)/2}}. \quad (113)$$

For Coulomb interactions between $\rho_{\mu\nu}(G)$ and $\rho_{\kappa}(G)$, we can derive the E_{cut} error,

$$\begin{aligned} \varepsilon(E_{\text{cut}}) &< 16\pi^2 \int_{\sqrt{2E_{\text{cut}}}}^{\infty} \rho_{\mu\nu}(G) \rho_{\kappa}(G) dG \\ &\approx \frac{32\pi^2 N_{\mu} N_{\nu} N_{\kappa} e^{-\theta_{\mu\nu} d_{\mu\nu}^2}}{(2\alpha_{\mu\nu})^{l_{\mu\nu}-1} (2\alpha_{\kappa})^{l_{\kappa}}} \left(\frac{\pi^2}{\alpha_{\mu\nu} \alpha_{\kappa}} \right)^{\frac{3}{2}} (2E_{\text{cut}})^{\frac{l_{\mu\nu}+l_{\kappa}-1}{2}} e^{-\frac{E_{\text{cut}}}{2\theta_{\mu\nu\kappa}}} < \tau, \end{aligned} \quad (114)$$

where

$$\theta_{\mu\nu\kappa} = (\alpha_{\mu\nu}^{-1} + \alpha_{\kappa}^{-1})^{-1}.$$

I. Energy cutoff for nuclear attraction integrals

When calculating nuclear attraction integrals, we can use steep s-type Gaussian functions to mimic the charge distribution of point nuclear charges

$$\chi_\kappa = \sum_A \lim_{\zeta \rightarrow \infty} \left(\frac{\pi}{\zeta} \right)^{3/2} Z_A e^{-\zeta|r-R_A|^2}. \quad (115)$$

The three-center energy cutoff analysis (114) is ready to estimate E_{cut} for nuclear attraction integrals with the setting $l_\kappa = 0$ and $\alpha_\kappa \rightarrow \infty$

$$\varepsilon(E_{\text{cut}}) \lesssim \frac{32\pi^2 N_\mu N_\nu e^{-\theta_{\mu\nu} d_{\mu\nu}^2}}{(2\alpha_{\mu\nu})^{l_{\mu\nu}-1}} \left(\frac{\pi}{\alpha_{\mu\nu}} \right)^{\frac{3}{2}} (2E_{\text{cut}})^{\frac{l_{\mu\nu}-1}{2}} e^{-\frac{E_{\text{cut}}}{2\alpha_{\mu\nu}}} < \tau. \quad (116)$$

J. Energy cutoff for LR integrals

For LR integrals, energy cutoff is primarily determined by the Gaussian factor in the LR Coulomb kernel (12). Similar to the case of the full Coulomb kernel, we only need to consider the most compact orbital products in the system to estimate E_{cut} . By carrying out the analysis discussed in the previous sections, we obtain the truncation error as well as the E_{cut} inequality for the four-center LR integrals

$$\varepsilon(E_{\text{cut}}) < \frac{32\pi^2 \theta_{\mu\omega} (2E_{\text{cut}})^{2l_\mu-1}}{((4l_\mu-1)!!)^2} e^{-\frac{E_{\text{cut}}}{2\theta_{\mu\omega}}} < \tau \quad (117)$$

where

$$\theta_{\mu\omega} = (\alpha_\mu^{-1} + \omega^{-2})^{-1} \quad (118)$$

To ensure $((4l_\mu-1)!!$ has a meaningful value for all angular momentum l_μ , the convention $(-1)!! = 1$ is assumed.

For the three-center LR integrals, the E_{cut} estimator can be derived in a similar fashion

$$\varepsilon(E_{\text{cut}}) < \frac{32\pi^2 \theta_{\mu\mu\kappa\omega} 2^{l_\kappa+3/4} (2E_{\text{cut}})^{l_\mu+(l_\kappa-1)/2}}{(4l_\mu-1)!! \sqrt{(4l_\kappa-1)!!}} \left(\frac{\pi}{\alpha_\kappa} \right)^{\frac{3}{4}} e^{-\frac{E_{\text{cut}}}{2\theta_{\mu\mu\kappa\omega}}} < \tau. \quad (119)$$

IV. NUMERICAL TESTS AND DISCUSSION

A. Distance cutoff for overlap integrals

During the deviations for R_{cut} and E_{cut} , the factorization approximation (50) is widely applied almost in every integral. To measure the effectiveness of this approximation, we compared R_{cut} estimated by the overlap estimator (50) to the precise R_{cut} which is solved by a bisection search for the exact overlap integrals. Given angular momentum for bra and ket, we noticed that the relative error for R_{cut} only depends on the ratio between the Gaussian exponents of bra and ket. Table I summarizes the relative errors for various types of Gaussian basis functions. When the two basis functions have similar shapes (exponents ratio < 5), the R_{cut} errors are small (typically less than 3%). However, high angular momentum can slightly increase the error. When bra and ket have very different shapes, the errors can increase to around 10%. Nevertheless, the factorization approximation provides a good estimation for R_{cut} in overlap integrals.

B. Errors for ERIs

In an SCF calculation, the error of distance cutoff and energy cutoff estimations may be influenced by several factors, such as the basis set, size of unit cell, k-point mesh, Coulomb attenuation parameters. To evaluate the impact of these factors on the cutoff estimations, we computed ERIs with the range-separated algorithms and compared them to the benchmark data generated with the reciprocal-space formula (7) with very tight accuracy requirements ($\tau = 10^{-16}$).

Unless otherwise specified in each individual test, the test system has one s-type primitive Gaussian function with exponent $\alpha = 1.0$ inside a cubic cell with the edge length $a = 1.5$. The Coulomb attenuation parameter for range-separated algorithms is

TABLE I. Relative error for overlap integral distance cutoff estimation

l_μ	l_ν	$\alpha_\mu = \alpha_\nu$	$\alpha_\mu = 2\alpha_\nu$	$\alpha_\mu = 5\alpha_\nu$	$\alpha_\mu = 100\alpha_\nu$
0	0	0	0	0	0
0	1	0.003	0.005	0.007	0.028
0	2	0.006	0.009	0.015	0.058
0	3	0.009	0.013	0.022	0.093
0	4	0.012	0.017	0.029	0.134
1	0	0.003	0.002	0.001	0
1	1	0.007	0.007	0.009	0.026
1	2	0.010	0.011	0.015	0.053
1	3	0.012	0.015	0.022	0.084
1	4	0.015	0.019	0.028	0.120
2	0	0.006	0.005	0.003	0
2	1	0.010	0.009	0.010	0.025
2	2	0.012	0.013	0.016	0.050
3	0	0.009	0.007	0.004	0.001
3	1	0.012	0.011	0.011	0.024
3	2	0.015	0.015	0.017	0.048
4	4	0.022	0.024	0.030	0.102

set to $\omega = 0.5$. Gamma point is adopted for the integral computation. In the range-separated algorithm setups, we solve R_{cut} and E_{cut} for various precision requirements ($\tau = 10^{-5}$ to $\tau = 10^{-12}$) then transform R_{cut} and E_{cut} to lattice-sum range and plane-wave summation range using the transformation equations (33) and (36). They are used in the triple lattice-sum for the short-range part Eq. (15) and the summation over plane-waves for the long-range part Eq. (21).

We found that the accuracy is well-controlled in most tests in the sense that errors are reduced to a value near or slightly under the desired accuracy as we increase the precision requirements. It indicates that computational efforts are being properly utilized without being wasted on the unintended accuracy. Error underestimation is only observed in a few difficult configurations.

- The impact of lattice parameters is exhibited in Figure 1. In this test, we changed the cell edge length from $a = 1.0 \text{ \AA}$ to $a = 2.5 \text{ \AA}$. Generally, small cells lead to larger errors than big cells. Good accuracy can be achieved with moderate precision settings up to 10^{-10} . When the required precision is tighter than 10^{-11} , one may only achieve 10^{-10} accuracy for the cell with edge length $a = 1.0 \text{ \AA}$. One possible reason of the error is the numerical uncertainties in the underlying integral library³². To confirm that the error is not caused by approximations in cutoff estimators, we manually increased the value of R_{cut} and E_{cut} and found that the accuracy was not improved with larger values of R_{cut} or E_{cut} . For the system $a = 1.0$ at $\tau = 10^{-11}$, the triple lattice-sum in Eq. (15) involves about 1600^3 primitive SR-ERIs. Errors in individual primitive integrals, even the round-off error, can easily be accumulated to the magnitude around 10^{-10} .
- The k-point factor. Integrals $(\phi_\mu^{\mathbf{k}_1} \phi_\mu^{\mathbf{k}_2} | \phi_\mu^{\mathbf{k}_2} \phi_\mu^{\mathbf{k}_1})$ are computed for k-point grids $N_k = 1^3 \dots 4^3$ (Figure 2). We find similar accuracy performance in all k-point test cases. All calculations with various accuracy specifications can reach the required accuracy.
- Basis effects. We first tested the effects of basis function compactness by varying the Gaussian function exponent from $\alpha = 0.2$ to $\alpha = 5.0$ (Figure 3). For relatively compact basis functions, errors are reduced normally as we tighten the precision requirements. For diffused basis functions this trend only holds up to the precision around 10^{-9} . Errors may also be attributed to the numerical uncertainties in primitive integrals. For the basis function with $\alpha = 0.2$ at $\tau = 10^{-10}$, 1500^3 primitive SR-ERIs have to be included in the triple lattice-sum.

In the test for basis angular momentum effects, basis functions with angular momentum $l = 0 \dots 3$ are tested (Figure 4). The results show that the accuracy is manageable in all test cases, indicating that the angular momentum of a basis function is not a significant factor in the R_{cut} and E_{cut} estimation.

- In Figure 5, we show the errors for Coulomb attenuation parameters ($\omega = 0.2$ to $\omega = 2.0$). Similar to the trends we found in lattice parameter tests and basis function compactness tests, errors caused by small ω s are larger than errors of larger ω s. For small ω s, accuracy is limited around 10^{-10} because of numerical uncertainties. Cutoffs are slightly overestimated for large ω .

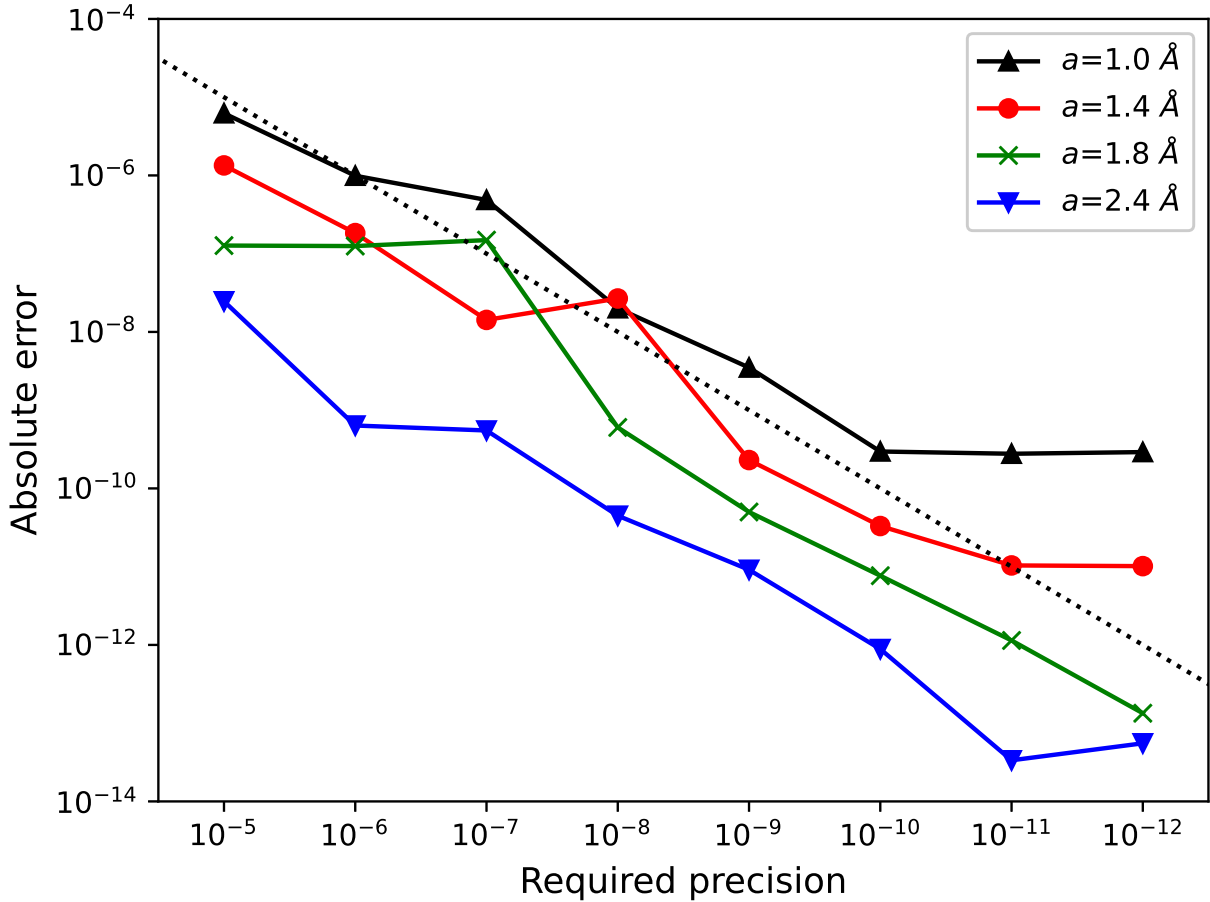


FIG. 1. Accuracy tests for lattice parameters

V. CONCLUSIONS

In this work, we provide a comprehensive analysis of the integral upper bound and cutoff estimators for the integral algorithms implemented in PySCF. The distance and energy cutoff estimators derived from the upper bound estimation are shown to be accurate enough to achieve the required accuracy for the range-separated integral algorithms while ensuring that computational resources are efficiently utilized. Our numerical tests show that the estimators are stable and reliable for various factors in routine crystalline calculations, such as k-point meshes, basis sets, unit cell sizes, and Coulomb attenuation parameters. Uncertainties around 10^{-9} may be encountered in certain cases when involving diffused basis functions, small unit cells, or small Coulomb attenuation parameters. Based on the integral estimation derived in this work, we expect that more aggressive optimization for crystalline integral programs can be carried out. Comprehensive algorithm and integral screening schemes will need to be designed. Additional technical details will be considered in future work.

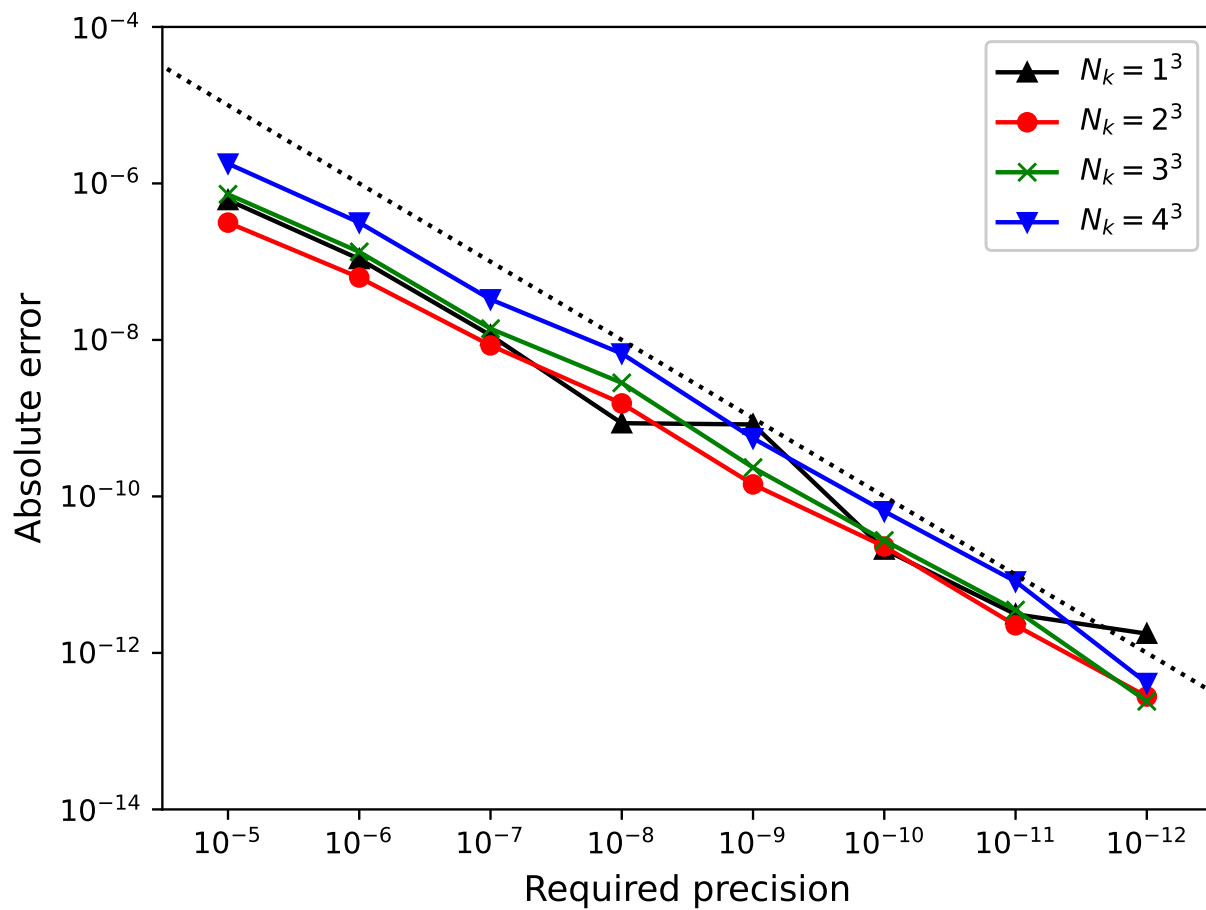


FIG. 2. Accuracy tests for k-points

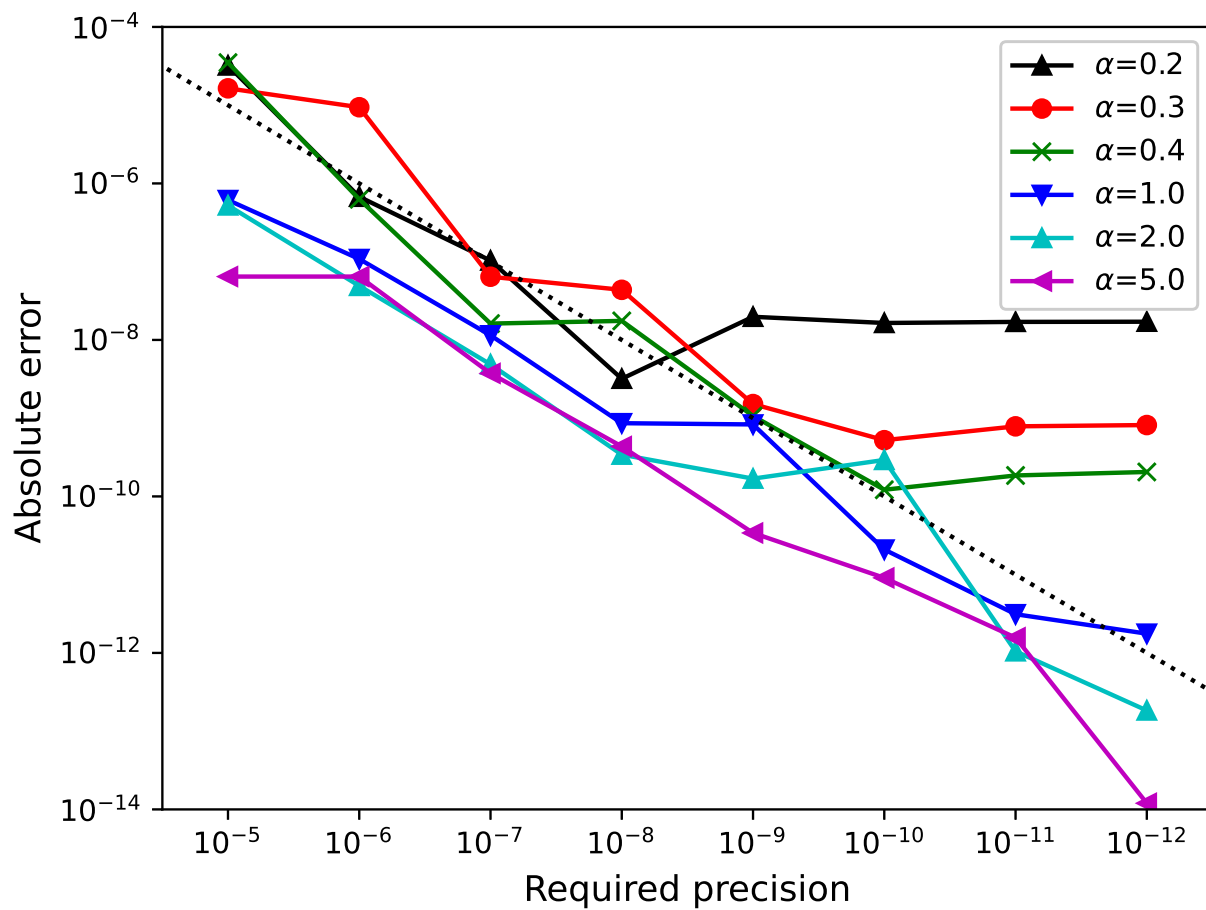


FIG. 3. Accuracy tests for exponents of Gaussian basis

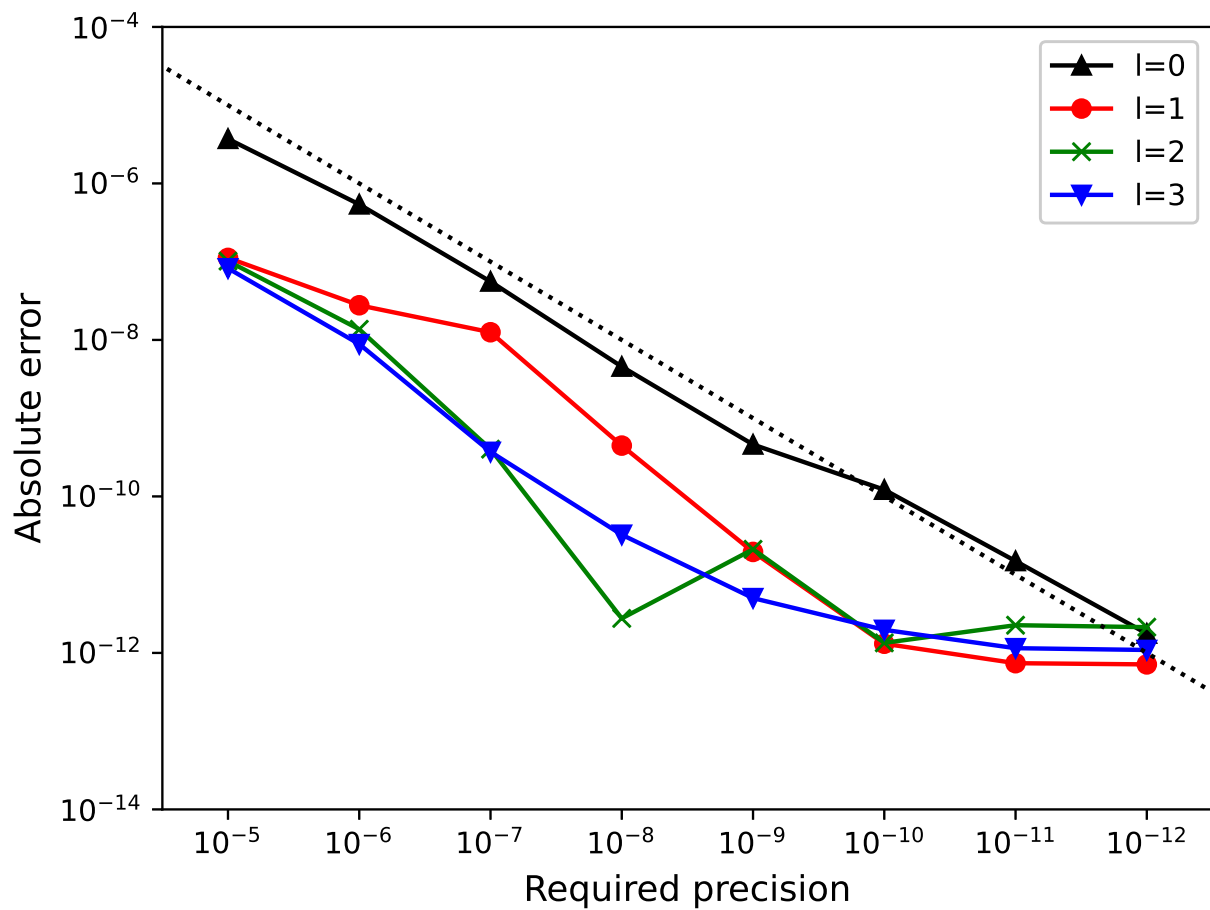


FIG. 4. Accuracy tests for angular momentum of Gaussian basis

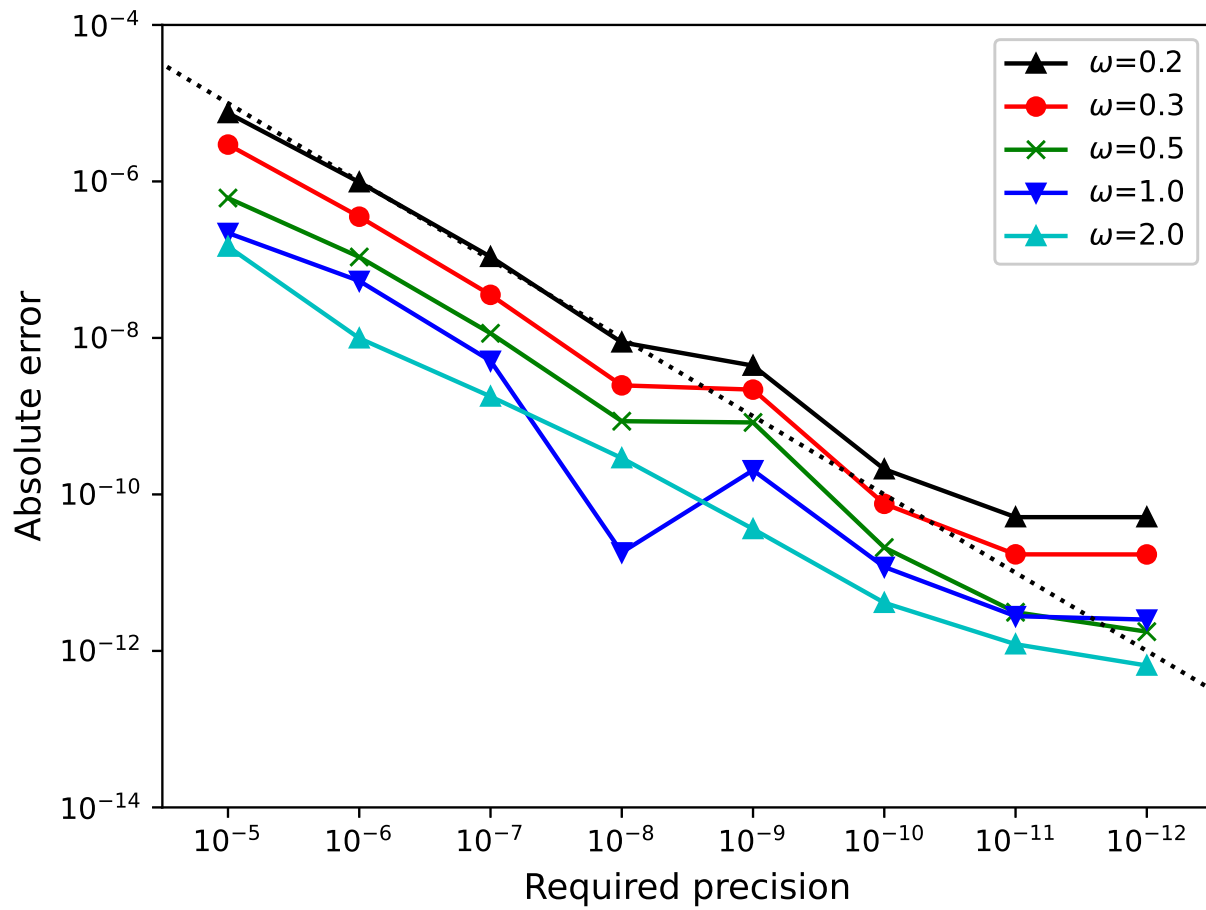


FIG. 5. Accuracy tests for Coulomb attenuation parameters

¹Q. Sun, T. C. Berkelbach, N. S. Blunt, G. H. Booth, S. Guo, Z. Li, J. Liu, J. D. McClain, E. R. Sayfutyarova, S. Sharma, S. Wouters, and G. K.-L. Chan, “Pyscf: the python-based simulations of chemistry framework,” *WIREs Comput Mol Sci* **8**, e1340 (2018).

²Q. Sun, X. Zhang, S. Banerjee, P. Bao, M. Barbry, N. S. Blunt, N. A. Bogdanov, G. H. Booth, J. Chen, Z.-H. Cui, J. J. Eriksen, Y. Gao, S. Guo, J. Hermann, M. R. Hermes, K. Koh, P. Koval, S. Lehtola, Z. Li, J. Liu, N. Mardirossian, J. D. McClain, M. Motta, B. Mussard, H. Q. Pham, A. Pulkin, W. Purwanto, P. J. Robinson, E. Ronca, E. R. Sayfutyarova, M. Scheurer, H. F. Schurkus, J. E. T. Smith, C. Sun, S.-N. Sun, S. Upadhyay, L. K. Wagner, X. Wang, A. White, J. D. Whitfield, M. J. Williamson, S. Wouters, J. Yang, J. M. Yu, T. Zhu, T. C. Berkelbach, S. Sharma, A. Y. Sokolov, and G. K.-L. Chan, “Recent developments in the pyscf program package,” *J. Chem. Phys.* **153**, 024109 (2020).

³J. Hutter, M. Iannuzzi, F. Schiffmann, and J. VandeVondele, “cp2k: atomistic simulations of condensed matter systems,” *WIREs Computational Molecular Science* **4**, 15–25 (2014), <https://wires.onlinelibrary.wiley.com/doi/pdf/10.1002/wcms.1159>.

⁴T. D. Kühne, M. Iannuzzi, M. Del Ben, V. V. Rybkin, P. Seewald, F. Stein, T. Laino, R. Z. Khalilullin, O. Schütt, F. Schiffmann, D. Golze, J. Wilhelm, S. Chulkov, M. H. Bani-Hashemian, V. Weber, U. Borštník, M. Taillefumier, A. S. Jakobovits, A. Lazzaro, H. Pabst, T. Müller, R. Schade, M. Guidon, S. Andermatt, N. Holmberg, G. K. Schenter, A. Hehn, A. Bussy, F. Belleflamme, G. Tabacchi, A. Glöß, M. Lass, I. Bethune, C. J. Mundy, C. Plessl, M. Watkins, J. VandeVondele, M. Krack, and J. Hutter, “Cp2k: An electronic structure and molecular dynamics software package - quickstep: Efficient and accurate electronic structure calculations,” *J. Chem. Phys.* **152**, 194103 (2020).

⁵A. Erba, J. K. Desmarais, S. Casassa, B. Civalleri, L. Donà, I. J. Bush, B. Searle, L. Maschio, L. Edith-Daga, A. Cossard, C. Ribaldone, E. Ascrizzi, N. L. Marana, J.-P. Flament, and B. Kirtman, “Crystal23: A program for computational solid state physics and chemistry,” *J. Chem. Theory Comput.* (2022), 10.1021/acs.jctc.2c00958.

⁶P. M. W. Gill, B. G. Johnson, and J. A. Pople, “A simple yet powerful upper bound for coulomb integrals,” *Chemical Physics Letters* **217**, 65–68 (1994).

⁷D. S. Lambrecht, B. Doser, and C. Ochsenfeld, “Rigorous integral screening for electron correlation methods,” *J. Chem. Phys.* **123**, 184102 (2005).

⁸S. A. Maurer, D. S. Lambrecht, D. Flraig, and C. Ochsenfeld, “Distance-dependent schwarz-based integral estimates for two-electron integrals: Reliable tightness vs. rigorous upper bounds,” *J. Chem. Phys.* **136**, 144107 (2012).

⁹S. A. Maurer, D. S. Lambrecht, J. Kussmann, and C. Ochsenfeld, “Efficient distance-including integral screening in linear-scaling møller-plesset perturbation theory,” *J. Chem. Phys.* **138**, 014101 (2013).

¹⁰D. S. Hollman, H. F. Schaefer, and E. F. Valeev, “A tight distance-dependent estimator for screening three-center coulomb integrals over gaussian basis functions,” *J. Chem. Phys.* **142**, 154106 (2015).

¹¹E. F. Valeev and T. Shiozaki, “Comment on ‘a tight distance-dependent estimator for screening three-center coulomb integrals over gaussian basis functions’ [j. chem. phys. 142, 154106 (2015)],” *J. Chem. Phys.* **153**, 097101 (2020).

¹²A. F. Izmaylov, G. E. Scuseria, and M. J. Frisch, “Efficient evaluation of short-range hartree-fock exchange in large molecules and periodic systems,” *J. Chem. Phys.* **125**, 104103 (2006).

¹³T. H. Thompson and C. Ochsenfeld, “Integral partition bounds for fast and effective screening of general one-, two-, and many-electron integrals,” *J. Chem. Phys.* **150**, 044101 (2019).

¹⁴G. Lippert, J. Hutter, and M. Parrinello, “The gaussian and augmented-plane-wave density functional method for ab initio molecular dynamics simulations,” *Theor. Chem. Acc.* **103**, 124–140 (1999).

¹⁵P. Čársky, R. Čurík, and v. Varga, “Efficient evaluation of coulomb integrals in a mixed gaussian and plane-wave basis using the density fitting and cholesky decomposition,” *J. Chem. Phys.* **136**, 114105 (2012).

¹⁶M. D. Ben, J. Hutter, and J. VandeVondele, “Electron correlation in the condensed phase from a resolution of identity approach based on the gaussian and plane waves scheme,” *J. Chem. Theory Comput.* **9**, 2654–2671 (2013), <http://dx.doi.org/10.1021/ct4002202>.

¹⁷A. M. Burow, M. Sierka, and F. Mohamed, “Resolution of identity approximation for the coulomb term in molecular and periodic systems,” *J. Chem. Phys.* **131**, 214101 (2009).

¹⁸K. N. Kudin and G. E. Scuseria, “Linear-scaling density-functional theory with gaussian orbitals and periodic boundary conditions: Efficient evaluation of energy and forces via the fast multipole method,” *Phys. Rev. B* **61**, 16440–16453 (2000).

¹⁹L. Maschio and D. Usyat, “Fitting of local densities in periodic systems,” *Phys. Rev. B* **78**, 073102 (2008).

²⁰C. Pisani, L. Maschio, S. Casassa, M. Halo, M. Schütz, and D. Usyat, “Periodic local mp2 method for the study of electronic correlation in crystals: Theory and preliminary applications,” *J. Comput. Chem.* **29**, 2113–2124 (2008).

²¹D. Usyat, L. Maschio, F. R. Manby, S. Casassa, M. Schütz, and C. Pisani, “Fast local-mp2 method with density-fitting for crystals. ii. test calculations and application to the carbon dioxide crystal,” *Phys. Rev. B* **76**, 075102 (2007).

²²V. Varga, M. Milko, and J. Noga, “Density fitting of two-electron integrals in extended systems with translational periodicity: The coulomb problem,” *J. Chem. Phys.* **124**, 034106 (2006).

²³J. Spencer and A. Alavi, “Efficient calculation of the exact exchange energy in periodic systems using a truncated coulomb potential,” *Phys. Rev. B* **77**, 193110 (2008).

²⁴M. Guidon, J. Hutter, and J. VandeVondele, “Robust periodic hartree-fock exchange for large-scale simulations using gaussian basis sets,” *J. Chem. Theory Comput.* **5**, 3010–3021 (2009).

²⁵Q. Sun, T. C. Berkelbach, J. D. McClain, and G. K.-L. Chan, “Gaussian and plane-wave mixed density fitting for periodic systems,” *J. Chem. Phys.* **147**, 164119 (2017).

²⁶H.-Z. Ye and T. C. Berkelbach, “Fast periodic gaussian density fitting by range separation,” *J. Chem. Phys.* **154**, 131104 (2021).

²⁷H.-Z. Ye and T. C. Berkelbach, “Tight distance-dependent estimators for screening two-center and three-center short-range coulomb integrals over gaussian basis functions,” *J. Chem. Phys.* **155**, 124106 (2021).

²⁸H.-Z. Ye and T. C. Berkelbach, “Correlation-consistent gaussian basis sets for solids made simple,” *J. Chem. Theory Comput.* **18**, 1595–1606 (2022).

²⁹Q. Sun, “Exact exchange matrix of periodic hartree-fock theory for all-electron simulations,” arXiv:2012.07929 [physics.chem-ph] (2020), arXiv:2012.07929 [chem-ph].

³⁰S. J. Bintrim, T. C. Berkelbach, and H.-Z. Ye, “Integral-direct hartree-fock and møller-plesset perturbation theory for periodic systems with density fitting: Application to the benzene crystal,” *J. Chem. Theory Comput.* **18**, 5374–5381 (2022).

³¹S. Sharma, A. F. White, and G. Beylkin, “Fast exchange with gaussian basis set using robust pseudospectral method,” *J. Chem. Theory Comput.* **18**, 7306–7320 (2022).

³²Q. Sun, “Libcint: An efficient general integral library for gaussian basis functions,” *J. Comput. Chem.* **36**, 1664–1671 (2015).